

STUDY ON THE FORMATION MECHANISM OF SECONDARY EPFRS IN ATMOSPHERIC PARTICULATE MATTER EXPOSED TO SUNLIGHT

Qin WH^{1,2}, Ai J^{1,2}, Cheng SM^{1,2}, Chen J^{1,2,*}

¹State Key Joint Laboratory of Environment Simulation and Pollution Control, School of Environment, Beijing Normal University, Beijing, China, 100875, 202021180048@mail.bnu.edu.cn; ²Center of Atmospheric Environmental Studies, Beijing Normal University, Beijing, China, 100875

1. Introduction

Environmentally persistent free radicals (EPFRs) are a type of long-lived organic free radicals that can exist in the environment for tens of days or even months^{1,2,3}. EPFRs can catalyze the production of reactive oxygen species (ROS) in the human body, such as superoxide anion free radicals ($\cdot\text{O}_2^-$), hydrogen peroxide (H_2O_2) and hydroxyl radicals (OH), which cause oxidative stress in the body and induce aging and diseases^{4,5}. In addition, EPFRs can also release ROS such as hydroxyl free radicals in aqueous solution⁶, which means that EPFRs may become a reservoir of active free radicals such as atmospheric OH, and participate in atmospheric free radical formation under high humidity conditions.

EPFRs are mainly produced on the surface of the formed metal particles under high temperature conditions through the transfer of electrons between organic matter and transition metal particles such as Fe, Cu, Zn, and Mn. In the atmospheric environment, EPFRs are also formed in heterogeneous reactions without transition metals. Chemical reactions (such as cloud and fog reactions, night reactions, etc.) promote the aging of atmospheric aerosols and the formation of secondary organic aerosols (SOA)⁷. However, the formation mechanism of secondary EPFRs in the atmosphere and the influencing mechanism of atmospheric active components remain to be explored.

2. Materials and methods

2.1 Materials

The materials used in the experiments are shown in the table 1.

Table 1. Materials in the sunlight exposure experiment and simulated sunlight exposure experiment.

Experiment	Sample Year	Sample Area	Sample Period	Particle size	Sample Number
Sunlight Exposure	2019	Beijing Urban Area	Non-heating period + heating period	$\frac{\text{PM}_1}{\text{PM}_{2.5}}$ PM ₁₀	40
	2020	Shanxi Rural Area	Non-heating period + heating period	PM _{2.5}	
Simulated Sunlight Exposure	2020	Beijing Urban area	Non-heating period + heating period	PM _{2.5}	31
	2020	Shanxi Urban Area	Non-heating period + heating period	PM _{2.5}	31

Among the samples under study, the non-heating period in Beijing covered 2019.11.1-2019.11.13, and the heating period covered 2019.11.14-2019.11.30. The non-heating periods in the rural area in Shanxi were 2020.2.10.-2020.2.17 and 2020.3.14-2020.3.19, and the heating periods were 2020.4.14.-2020.4.17 and 2020.4.21.-2020.5.4. The heating period of Shanxi (Yuncheng) urban area was 2020.11.1-2020.11.9, and the heating period was 2020.11.14.-2020.12.11.

2.2 Methods

In the sunlight exposure experiments, a 0.2cm×5cm strip-shaped quartz film sample loaded with particles was placed in a transparent membrane box, with the particle-loaded side exposed to sunlight. The sunlight exposure experiments were carried out on the roof of the School of Environment building, Beijing Normal University (39.96°N, 116.36°E) in September 2020 during the sunny days. The samples were continuously exposed to sunlight from 8:00 to 18:00, and then quickly measured by ESR. The difference between the concentration of EPFRs in the particulate matter after exposure to sunlight and the concentration of EPFRs in the corresponding sample that was not exposed to sunlight was determined as the concentration of generated EPFRs after sunlight exposure.

The simulated sunlight exposure experiment was carried out in a custom-made dark box. The entire system included the dark box, xenon lamp, sample tray and power supply. For each sample, three samples of 0.2cm×5cm particle-loaded quartz film were exposed to simulated sunlight. The light lasted for 15 minutes, then the ESR was

used to quickly determine the EPFR signals. The secondary generation of EPFRs was calculated in the same way as in the sunlight exposure experiment. Three parallel experiments were performed for each sample to reduce accidental errors.

3. Results and discussion

3.1 Decay intensity characteristics of EPFRs in different particulates under sunlight exposure

Figure 1 shows the attenuation characteristics of EPFRs in different particle sizes in the non-heating period and heating period of Beijing urban area in 2019 and Shanxi rural area in 2020 under sunlight. The results showed that the concentration of EPFRs increased significantly after the particulate matter was exposed to sunlight, indicating that the secondary generation of EPFRs was formed by the photochemical reaction of particulate matter under sunlight. In addition, the formation of secondary EPFRs in particles may also be affected by particle size and source. For the particulate matter collected in Beijing urban area, under 10-20 hours of sunlight, the EPFRs in PM₁, PM_{2.5} and PM₁₀ during the non-heating period increased by 181.2%, 142.1% and 61.6%, indicating that the secondary generation of EPFRs was enhanced in fine particles. However, the EPFRs of PM₁₀ in Beijing urban heating period increased by about 87.5% under sunlight, which was 8.3 times of the increase of EPFRs in fine particles, which indicated that secondary EPFRs were more likely in coarse particles during heating period. This may be due to the different sources of particulate matter. In addition, the variation trend in the rural area of Shanxi was contrary to those in Beijing urban area. The generation of secondary EPFRs was not observed during the non-heating period; while during the heating period, the generation of secondary EPFRs was around 33.5%, about 3 times of that of the Beijing urban area in the same period. This may be due to the fact that the carbon content of PM_{2.5} in Shanxi rural area during the heating period was much higher than that in Beijing urban area. In the next 80 hours of sunlight, the EPFRs in the particulates decreased rapidly, indicating that the secondary EPFRs have poor chemical stability⁸.

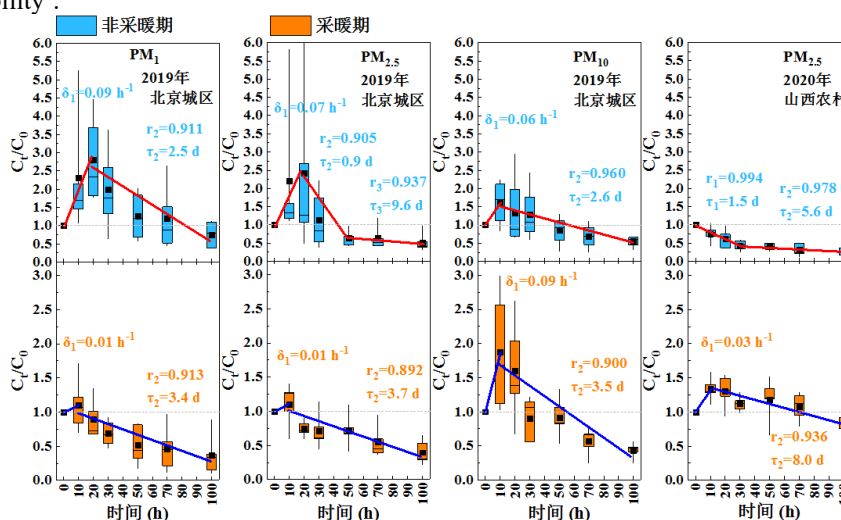


Figure 1. Decay characteristics of EPFRs in particulates with different particle sizes during non-heating and heating periods in Urban Beijing in 2019 and in Rural Shanxi in 2020 under sunlight irradiation.

3.2 Decay characteristics of g-factor and ΔH_{p-p} of EPFRs in different particulates under sunlight exposure

Figure 2 shows the g-factor and ΔH_{p-p} attenuation characteristics of EPFRs in atmospheric particulates with different particle sizes during the non-heating period and the heating period in the urban area of Beijing in 2019 and rural area in Shanxi in 2020. After 10-20 hours of sunlight exposure, the average of the maximum increase of g-factor of EPFRs in the non-heating period of Beijing urban area in 2019 for PM₁, PM_{2.5}, and PM₁₀ was 0.0002, 0.0003, and 0.0002, respectively; while during the heating period was 0.0001, 0.0002 and 0.0000, respectively. The above results indicate that for the secondarily generated EPFRs in the non-heating period, free radicals centered on oxygen or free radicals with oxygen heteroatoms centered on carbon were more likely to be formed. In Shanxi rural area, the maximum increase in the average g-factor of EPFRs in PM_{2.5} during non-heating and heating periods was 0.0001 and 0.0003, respectively, showing larger increase in the heating period than non-heating period. Previous studies have shown that a slight increase in g-factor represents an increase of the contribution of oxygen-centered free radicals in EPFRs, or the loss of more carbon-centered free radicals⁴. However, the g-factor of EPFRs in the next 80 hours of sunlight exposure showed a downward trend, which may be caused by the degradation of oxygen-containing EPFRs in particles due to continuous light. In addition, in the entire sunlight exposure experiment, ΔH_{p-p} increased first and then decreased, which was similar to the change of g-factor, and its value changed by 1.7 G, indicating that the types of total EPFRs in particle matter may have changed⁹.

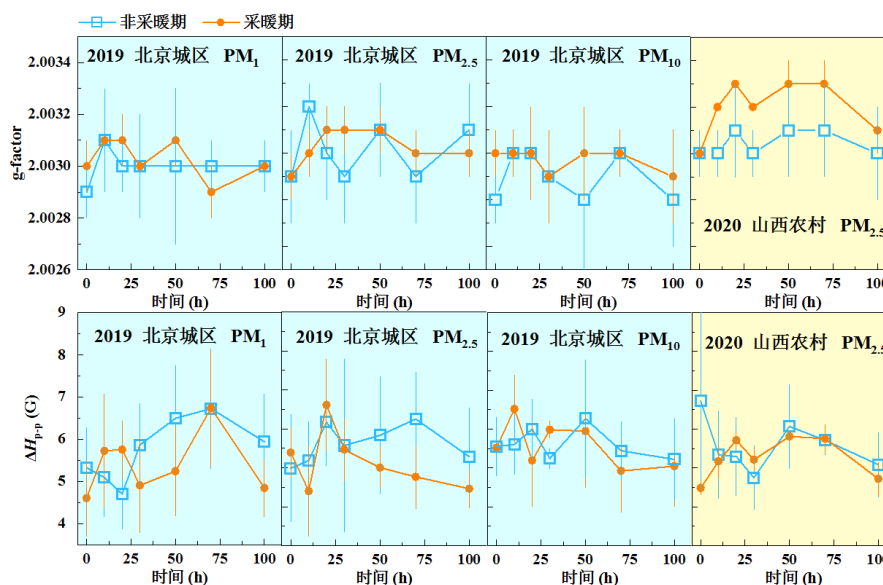


Figure 2. Decay characteristics of g-factor and ΔH_{p-p} of EPFRs in atmospheric particulates with different particle sizes in the non-heating period and heating period in Urban Beijing in 2019 and in Rural Shanxi in 2020

3.3 Decay characteristics of EFPFs in $PM_{2.5}$ under simulate sunlight exposure.

Figure 3 shows the EFPFRs and their corresponding g-factor and ΔH_{p-p} changes in the non-heating period and heating period of $PM_{2.5}$ in Beijing and Yuncheng in 2020 under simulate sunlight. The results showed that after $PM_{2.5}$ samples were exposed to simulated sunlight, the content of EFPFRs was significantly increased. Therefore, secondary EFPFRs in particles can be generated under visible light excitation¹⁰. However, the increase of EFPFRs in $PM_{2.5}$ varied in different regions. In 2020, $PM_{2.5}$ of the non-heating period in Beijing urban area and Yuncheng urban area increased by about 49% and 71% respectively after 15 minutes of simulated sunlight, while the EFPFRs in the heating period samples increased by about 40% and 47%, indicating the photochemistry of EFPFRs depended on the chemical composition of the particles. Moreover, the increase in EFPFRs in samples from Yuncheng urban area was greater than that in Beijing urban area, especially in samples from non-heating periods. The above results indicated that the samples from Yuncheng urban area, especially the $PM_{2.5}$ samples collected during the non-heating period, contained more components that can generate EFPFRs through photochemical action.

In addition, the g-factor and ΔH_{p-p} of the $PM_{2.5}$ samples changed before and after light, indicating that the type of secondary EFPFRs may be different from the EFPFRs in the original samples. After 15 minutes of light, the average g-factor of EFPFRs increased by about 0.0001, indicating that the secondary EFPFRs have a higher g-factor, which may be due to the formation of more oxygen-centered free radicals or free radicals centered on carbon and accompanied by oxygen atoms or other heteroatoms in the secondary EFPFRs. The average ΔH_{p-p} of EFPFRs increased by about 0.3-1.1G, further indicating that the types of secondary EFPFRs may be different from those in the original sample.

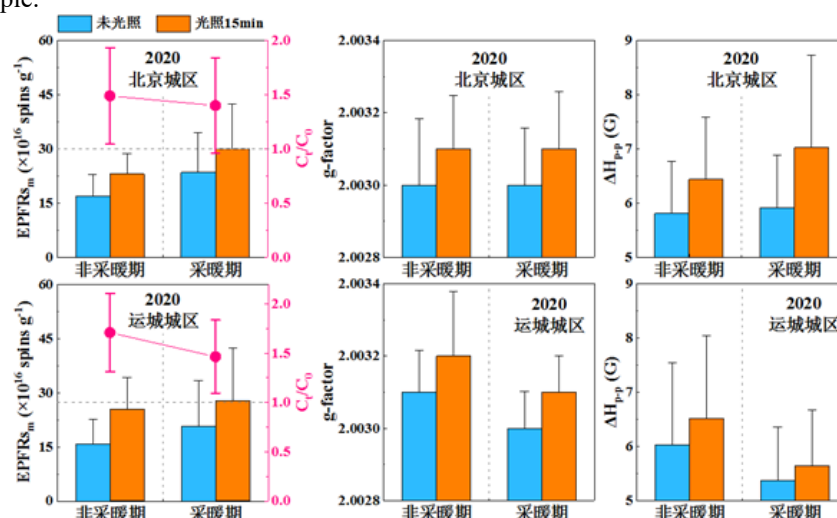


Figure 3. Decay characteristics of EFPFs and their corresponding g-factor and ΔH_{p-p} in $PM_{2.5}$ during non-heating period and heating period in Urban Beijing and Urban Yuncheng in 2020 under simulated sunlight irradiation.

3.4 Possible reasons for the increase of EPFRs

The formation process of secondary EPFRs in atmospheric particulate matter under sunlight exposure is very complicated. According to the report of Chen et al.⁸, HULIS-WSOC contributed 92% of the total secondary EPFRs generated under visible light irradiation, indicating that HULIS-WSOC may be an important particulate component of secondary EPFRs under light irradiation. In this study, in 2019, the mass concentration of WSOC and WSOC/OC in the particles in the non-heating period of Beijing urban area was obviously similar to the change of the secondary EPFR generation with the particle size. This may be reason for the different amounts of formation of secondary EPFRs in different particle sizes or in different periods. For the coarse particulate matter in Beijing urban area, the increase of secondary EPFRs during the non-heating period was about 25.9% less than that during the heating period, but there was basically no difference in the mass concentration of WSOC. This may be due to the higher content of POC in the particulate matter during the heating period. Therefore, it was inferred that WSOC-type organic carbon in particulate matter may contribute greatly to the formation of secondary EPFRs under visible light. In addition, different components of atmospheric particles can produce secondary EPFRs under simulated sunlight¹⁰. And organic matter mainly produces oxygen-centered free radicals, which may be the reason for the increase of g-factor of EPFRs after illumination.

4. Acknowledgements

This work was supported by National Natural Science Foundation of China (91543110), Fund of the Ministry of Science and Technology of the People's Republic of China (2019YFC0214203) and the APN (Asia-Pacific Network for Global Change Research) grant.

References

1. Chen QC, Sun HY, Wang MM, et al. (2018) *Environ. Sci. Technol.* 52, 9646-9655.
2. Gehling W and Dellinger B, (2013) *Environ. Sci. Technol.* 47, 8172-8178.
3. Yang LL, Liu GR, Zheng MH, et al. (2017) *Environ. Sci. Technol.* 51, 7936-7944.
4. Kelley MA., Hebert VY, Thibeaux TM, et al. (2013) *Chem. Res. Toxicol.* 26, 1862-1871.
5. 郭溪, 张瑛, 孟甜甜等, (2018) *环境化学* 37, 2095-2102.
6. Arangio AM, Tong H, Socorro J, et al. (2016) *Atmos. Chem. Phys.* 16, 13105-13119.
7. 王朋, 吴敏, 李浩等, (2017) *化工进展* 36, 4243-4249.
8. Chen QC, Sun HY, Wang MM, et al. (2019) *Environ. Sci Technol.* 53, 10053-10061.
9. Chen QC, Sun HY, Mu Z, et al. (2019) *Environ. Pollut.* 247, 18-26.